An eigenvalue method for open-boundary quantum transmission problems

Zhi-an Shao, Wolfgang Porod, and Craig S. Lent[a)]
Department of Electrical Engineering, University of Notre Dame, Notre Dame, Indiana 46556

David J. Kirkner
Department of Civil Engineering and Geological Sciences, University of Notre Dame, Notre Dame, Indiana 46556

(Received 22 February 1995; accepted for publication 27 April 1995)

We present a numerical technique for open-boundary quantum transmission problems which yields, as the direct solutions of appropriate eigenvalue problems, the energies of (i) quasi-bound states and transmission poles, (ii) transmission ones, and (iii) transmission zeros. The eigenvalue problem results from reducing the inhomogeneous transmission problem to a homogeneous problem by forcing the in-coming source term to zero. This homogeneous problem can be transformed to a standard linear eigenvalue problem. By treating either the transmission amplitude $t(E)$ or the reflection amplitude $r(E)$ as the known source term, this method also can be used to calculate the positions of transmission zeros and ones. We demonstrate the utility of this technique with several examples, such as single- and double-barrier resonant tunneling and quantum waveguide systems, including t-stubs and loops. © *1995 American Institute of Physics.*

I. INTRODUCTION

A common computational problem is to determine the quasi-bound states of a resonant transmitting quantum system. It is well known that the quasi-bound states of an open (leaky) system are related to the true bound states of the corresponding closed (isolated) system.[1] While it is well known that the true bound states may be obtained by solving an eigenvalue problem, there has been no direct way of computing the corresponding quasi-bound state energies. In this article, we present a technique which allows, by the direct solution of an eigenvalue problem, the computation of the positions and life times of quasi-bound states and the energies of transmission ones and zeros.

For an isolated system, the bound states satisfy the time-independent Schrödinger equation,

$$(\mathbf{H}-E\mathbf{D})\psi=0. \tag{1}$$

In discretized numerical form, the above equation represents a vector equation. Because the wave function at the boundary is zero, the Hamiltonian matrix $\mathbf{H}$ is Hermitian and the system has only bound states.

For an open system, the Hamiltonian matrix $\mathbf{H}$ is no longer Hermitian, hence the system possesses quasi-bound states.[2] As is customary, we model the open system as the previously isolated system connected to reservoirs by current-carrying leads,[3–5] schematically shown in Fig. 1. For a given energy E, the wave functions in the left- and right-hand side leads are plane waves with wave numbers k_L and k_R, respectively. The resulting complex-valued boundary conditions render the system's Hamiltonian matrix non-Hermitian.

The prototypical transmission problem is schematically shown in Fig. 1(a), where an in-coming flux with amplitude $a(E)$ (the "forcing term") leads to out-going transmitted and reflected waves, with amplitudes $t(E)$ and $r(E)$, respectively (the "system response"). As will be shown in Section II [Eq. (22)], the unknown system wave function is given as the solution of the following inhomogeneous problem,

$$(\mathbf{H}-k_L\mathbf{B}^L-k_R\mathbf{B}^R-E\mathbf{D})\boldsymbol{\psi}=-a(E)\mathbf{P}. \tag{2}$$

The left-hand side contains the matrices $\mathbf{H}$ and $\mathbf{D}$, which are the same as for the corresponding bound-state problem, and which is obtained by setting the wave function to zero at the boundaries, compare to Eq. (1). The current-carrying open-system boundary conditions are represented by the complex and sparse matrices $\mathbf{B}^L$ and $\mathbf{B}^R$; in fact, they only possess a non-zero entry at the boundary. $\boldsymbol{\psi}$ is the unknown wave function vector which can be used to calculate the amplitudes $t(E)$ [and $r(E)$]. The right-hand side contains the forcing term, $a(E)\mathbf{P}$. For any given amplitude of the in-coming flux, $a(E)$, the solution of the system is uniquely determined.

Quasi-bound states are characterized by a complex energy, $E=E_R-i\Gamma$, where the real part E_R gives the energy of the resonance and its imaginary part Γ is related to the lifetime τ by $\tau=\hbar/(2\Gamma)$.[6] It is well known that quasi-bound states lead to poles of the propagator (and the transmission amplitude),[7] and therefore one can solve Eq. (2) in the complex-energy plane to locate the position of the poles. Another way to find these poles is to search for the zero of the determinant of the coefficient matrix $\det(\mathbf{H}-k_L\mathbf{B}^L-k_R\mathbf{B}^R-E\mathbf{D})=0$; a zero of the determinant means that Eq. (2) has no nontrivial solution, or $\boldsymbol{\psi}$ [or $t(E)$] possesses poles. Usually, this can be done by numerical search techniques, such as a Newton iteration method.[8,9]

In this article, we present a direct solution method which yields the complex-valued quasi-bound state energies as the solutions of a conventional linear eigenvalue problem. Searching for the zeros of the system determinant of the inhomogeneous problem (2), is equivalent to finding the eigenvalues of the corresponding homogeneous problem,

$$(\mathbf{H}-k_L\mathbf{B}^L-k_R\mathbf{B}^R-E\mathbf{D})\boldsymbol{\psi}=0. \tag{3}$$

[a)]Electronic mail: lent@callisto.ee.nd.edu

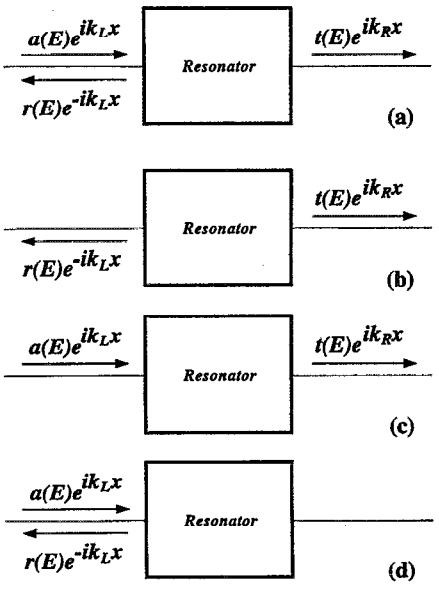

FIG. 1. Schematic diagram of a resonant transmitting structure coupled to two leads; (a) shows an incident wave from the left with its transmitted and reflected components; (b) shows no incident wave from the left (transmission poles); (c) shows no reflected wave in the left (transmission ones); (d) shows no transmitted wave in the right (transmission zeros).

In general, this is a highly non-linear eigenvalue problem since **H** depends both upon k and E. For example, if we expand the wave function in terms of plane waves, then the matrix **H** contains terms which are exponential in the wave number [$\propto \exp(ikx)$], and Eq. (3) cannot be solved by standard eigenvalue routines. However, using the finite element method,[10] the unknown wave function is expanded by linear shape functions, and the coefficient matrix of Eq. (3) becomes a quadratic function of the wave number k. As we will show below, one can then transform this quadratic nonlinear matrix equation into a linear eigenvalue problem with increased matrix dimension.

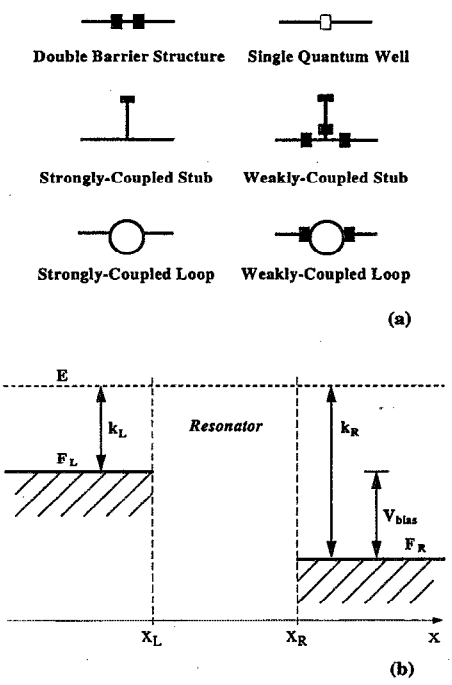

FIG. 2. Schematic diagram of resonant transmission systems and their potential profile for a given bias; (a) shows some typical resonant structures; (b) shows a resonant transmission system with an applied bias.

The transition from the above inhomogeneous problem (2) to the homogeneous problem has a geometric interpretation: The homogeneous problem is obtained by setting the incoming forcing term to zero, as schematically depicted in Fig. 1(b). The eigen-states of (3) are the quasi-bound states which "leak out" on both sides of the open system.

Using an argument similar to the above treatment, we can also view the transmitted (or reflected) waves as the forcing terms; $t(E)$ or $r(E)$ would then be the known variable in Eq. (2). Replacing $a(E)$ on the right-hand side of Eq. (2) by either one of them (and moving $a(E)$ as the now unknown variable onto the left-hand side), we obtain linear inhomogeneous problems similar to Eq. (2). It is obvious that the solutions of these new problems correspond to either transmission ones ($t=1$ and $r=0$), see Fig. 1(c), or transmission zeros ($t=0$ and $r=1$), see Fig. 1(d).

From a mathematical viewpoint, there are $(n+1)$ variables but only n equations in (2). We can choose any one of them as the known variable, and then the rest of the system is uniquely determined. Forcing this known (or source) variable to zero, leads to an eigenvalue problem. The three cases of interest are:

(1) transmission poles [$a(E)\equiv 0$],
(2) transmission ones [$r(E)\equiv 0$], and
(3) transmission zeros [$t(E)\equiv 0$].

This article is organized as follows: In Sec. II, we formulate the inhomogeneous problem for transmission; in Sec. III, we formulate the eigenvalue problem for transmission poles for cases with and without bias; in Sec. IV, we formulate the eigenvalue problem for transmission ones; in Sec. V, we formulate the eigenvalue problem for transmission zeros; in Sec. VI, we apply this eigenvalue method to several examples to demonstrate its utility. Finally, we summarize and give concluding comments.

II. TRANSMISSION PROBLEM

A. Formulation

In this section, we formulate the inhomogeneous problem for transmission in quasi-one-dimensional quantum waveguide systems, which are schematically shown in Fig. 2(a). These structures include double-barrier and single quantum well structures, t-stubs, and loops. The one-dimensional effective mass Schrödinger equation,

$$-\frac{\hbar^2}{2}\frac{\partial}{\partial x}\left(\frac{1}{m^*}\frac{\partial\psi}{\partial x}\right)+V\psi=E\psi, \tag{4}$$

has to be solved for the problem domain $[x_L, x_R]$.

The wave functions in the asymptotic regions on the left and right are

$$\psi_L(x,E)=a(E)\exp(ik_Lx)+r(E)\exp(-ik_Lx), \tag{5a}$$

$$\psi_R(x,E)=t(E)\exp(ik_Rx). \tag{5b}$$

The amplitude of the in-coming plane wave with energy E is denoted by $a(E)$. The resulting reflection and transmission amplitudes are denoted by $r(E)$ and $t(E)$, respectively.

Using an effective-mass model, the energy E is related to the wave number k by [see Fig. 2(b)],

$$k_L=\frac{\sqrt{2m_L^*(E-F_L)}}{\hbar}, \tag{6a}$$

$$k_R=\frac{\sqrt{2m_R^*(E-F_R)}}{\hbar}. \tag{6b}$$

Here, m_i^* is the effective mass of the carrier $(i=L,R)$. The Fermi energies on the left- and right-hand sides, denoted by F_L and F_R, respectively, are related to the external bias V_{bias} by

$$F_L-F_R=eV_{\text{bias}}, \tag{7}$$

e is electronic charge. Note that the wave numbers k_L and k_R are given by the carrier energy E and the applied bias V_{bias}.

The transmission and reflection amplitudes $t(E)$ and $r(E)$ are obtained from the wave functions ψ_R and ψ_L by

$$t(E)=\psi_R(x_R,E)e^{-ik_Rx_R}, \tag{8a}$$

$$r(E)=[\psi_L(x_L,E)-e^{ik_Lx_L}]e^{ik_Lx_L}, \tag{8b}$$

with x_L being the left-hand boundary of the system and x_R the right-hand boundary.

At the two edges of the system, we have the following boundary conditions by matching the wave function and its derivative to plane waves on both sides,[5]

$$\psi(x_L)=ae^{ik_Lx_L}+re^{-ik_Lx_L}, \tag{9a}$$

$$\begin{aligned}\psi'(x_L)&=ik_L(ae^{ik_Lx_L}-re^{-ik_Lx_L})\\&=2ik_Lae^{ik_Lx_L}-ik_L\psi(x_L),\end{aligned} \tag{9b}$$

$$\psi(x_R)=te^{ik_Rx_R}, \tag{9c}$$

$$\psi'(x_R)=ik_Rte^{ik_Rx_R}=ik_R\psi(x_R). \tag{9d}$$

Note that the wave functions at the boundaries are related to the transmission amplitude $t(E)$ and the reflection amplitude $r(E)$.

B. Finite element discretization

Equations (4), (9b), and (9d) constitute a boundary value problem for the wave function, $\psi(x)$, on the problem domain $[x_L,x_R]$. In this section we develop a weak variational statement of this problem and a finite dimensional approximation by the finite element method.

Multiplying Eq. (4) by an arbitrary test function ϕ (assumed sufficiently smooth), and integrating over the problem domain yields,

$$\int_{x_L}^{x_R}\left[\frac{\partial}{\partial x}\left(\frac{1}{m^*(x)}\frac{\partial\psi}{\partial x}\right)\phi+\frac{2}{\hbar^2}(E-V)\psi\phi\right]dx=0. \tag{10}$$

Integration of Eq. (10) by parts then gives

$$\frac{1}{m_R^*}\psi'(x_R)\phi(x_R)-\frac{1}{m_L^*}\psi'(x_L)\phi(x_L)-\int_{x_L}^{x_R}\frac{1}{m^*(x)}\psi'\phi'\,dx+\frac{2}{\hbar^2}\int_{x_L}^{x_R}(E-V)\psi\phi\,dx=0. \tag{11}$$

Using Eqs. (9b) and (9d) results in

$$\underline{\underline{\frac{i}{m_R^*}k_R\psi(x_R)\phi(x_R)}}+\underline{\underline{\frac{i}{m_L^*}k_L\psi(x_L)\phi(x_L)}}-\left(\int_{x_L}^{x_R}\frac{1}{m^*(x)}\psi'\phi'\,dx+\frac{2}{\hbar^2}\int_{x_L}^{x_R}V\psi\phi\,dx\right)+E\frac{2}{\hbar^2}\int_{x_L}^{x_R}\psi\phi\,dx=\underline{\underline{\frac{2i}{m_L^*}k_La(E)\phi(x_L)e^{ik_Lx_L}}}. \tag{12}$$

We now state the weak variational problem equivalent to the boundary value problem defined by Eqs. (4), (9b), and (9d).

Problem: Find $\psi(x)$ on $[x_L,x_R]$ such that Eq. (4) is satisfied for all test functions ϕ. This formulation of the problem will form the basis of our solution method. Note that the open boundary conditions introduce the terms proportional to k in Eq. (4), i.e., the first two terms on the left-hand side and the right-hand side term. These terms, which are underlined for clarity, would be zero for the bound-state problem.

We now develop a finite dimensional approximation to the above variational problem by the finite element method. We first discretize the solution domain with n nodal points with coordinates x_i, where $x_1=x_L$ and $x_n=x_R$. We expand the wave function ψ and the test function ϕ in terms of linear shape functions U_i as,

$$\psi(x)=\sum_{i=1}^{n}\psi_iU_i(x), \tag{13a}$$

$$\phi(x)=\sum_{i=1}^{n}\phi_iU_i(x), \tag{13b}$$

where ψ_i and ϕ_i are the function values at the nodal point x_i; the shape functions have the property that $U_j(x_i)=\delta_{ij}$.[10] The vector containing the values of the wave function at the nodal points is denoted by ψ, such that $\psi_j=\psi(x_j)$. With this, we have

$$\psi(x_R)=\psi_n,\quad \phi(x_R)=\phi_n, \tag{14a}$$

$$\psi(x_L)=\psi_1,\quad \phi(x_L)=\phi_1. \tag{14b}$$

The discretized form of the weak variational form of the Schrödinger Eq. (12) becomes

$$\underline{\underline{\frac{i}{m_R^*}k_R\psi(x_R)\phi(x_R)}}+\underline{\underline{\frac{i}{m_L^*}k_L\psi(x_L)\phi(x_L)}}$$
$$-\sum_{j=1}^{n}\phi_j\sum_{i=1}^{n}\psi_i\int_{x_L}^{x_R}\frac{1}{m^*(x)}U_i'U_j'\,dx$$
$$+E\frac{2}{\hbar^2}\sum_{j=1}^{n}\phi_j\sum_{i=1}^{n}\psi_i\int_{x_L}^{x_R}U_iU_j\,dx$$
$$-\frac{2}{\hbar^2}\sum_{j=1}^{n}\phi_j\sum_{i=1}^{n}\psi_i\int_{x_L}^{x_R}VU_iU_j\,dx$$
$$=\underline{\underline{\frac{2i}{m_L^*}k_La(E)\phi(x_L)e^{ik_Lx_L}}}. \tag{15}$$

The above equation can also be written in the following form

$$\sum_{j=1}^{n}\phi_j\sum_{i=1}^{n}\psi_i\left(\underline{\underline{\frac{i}{m_R^*}k_R\delta_{in}\delta_{jn}}}+\underline{\underline{\frac{i}{m_L^*}k_L\delta_{i1}\delta_{j1}}}\right.$$
$$-\int_{x_L}^{x_R}\frac{1}{m^*(x)}U_i'U_j'\,dx+E\frac{2}{\hbar^2}\int_{x_L}^{x_R}U_iU_j\,dx$$
$$\left.-\frac{2}{\hbar^2}\int_{x_L}^{x_R}VU_iU_j\,dx\right)=\sum_{j=1}^{n}\phi_j\underline{\underline{\frac{2i}{m_L^*}k_La\delta_{j1}e^{ik_Lx_L}}}. \tag{16}$$

Since ϕ is an arbitrary test function, Eq. (16) must hold individually for each term ϕ_j in the sum with index j, which results in a set of n linear equations,

$$\begin{pmatrix}\left(W_{11}-\frac{ik_L}{m_L^*}\right) & W_{12} & 0 & 0 & 0\\ W_{21} & \ddots & \ddots & 0 & 0\\ 0 & \ddots & \ddots & \ddots & 0\\ 0 & 0 & \ddots & \ddots & W_{(n-1)n}\\ 0 & 0 & 0 & W_{n(n-1)} & \left(W_{nn}-\frac{ik_R}{m_R^*}\right)\end{pmatrix}$$
$$\times\begin{pmatrix}\psi_1\\ \psi_2\\ \vdots\\ \psi_{n-1}\\ \psi_n\end{pmatrix}=-a(E)\begin{pmatrix}\frac{2ik_Le^{ik_Lx_L}}{m_L^*}\\ 0\\ 0\\ \vdots\\ 0\end{pmatrix}, \tag{17}$$

where

$$\mathbf{W}=\mathbf{H}-E\mathbf{D}, \tag{18}$$

$$\mathbf{H}_{ij}=\int_{x_L}^{x_R}\frac{1}{m^*}U_i'U_j'\,dx+\frac{2}{\hbar^2}\int_{x_L}^{x_R}VU_iU_j\,dx, \tag{19}$$

$$\mathbf{D}_{ij}=\frac{2}{\hbar^2}\int_{x_L}^{x_R}U_iU_j\,dx. \tag{20}$$

Using the definitions

$$\psi^T=(\psi_1,\psi_2,\ldots,\psi_n), \tag{21a}$$

$$\mathbf{P}^T=\frac{2i}{m_L^*}k_Le^{ik_Lx_L}(1,0,\ldots,0), \tag{21b}$$

$$\mathbf{B}^L=\frac{i}{m_L^*}\begin{pmatrix}1&0&0&0&0\\0&0&\ddots&0&0\\0&\ddots&\ddots&\ddots&0\\0&0&\ddots&\ddots&0\\0&0&0&0&0\end{pmatrix}, \tag{21c}$$

$$\mathbf{B}^R=\frac{i}{m_R^*}\begin{pmatrix}0&0&0&0&0\\0&\ddots&\ddots&0&0\\0&\ddots&\ddots&\ddots&0\\0&0&\ddots&0&0\\0&0&0&0&1\end{pmatrix}. \tag{21d}$$

Equation (17) can be written as

$$(\mathbf{H}-\underline{\underline{k_L\mathbf{B}^L}}-\underline{\underline{k_R\mathbf{B}^R}}-E\mathbf{D})\boldsymbol{\psi}=-\underline{\underline{a(E)\mathbf{P}}}. \tag{22}$$

Note that there is only a single non-zero entry for both $\mathbf{B}^L$ and $\mathbf{B}^R$ which couple the solution domain to the left lead (node 1) and right lead (node n).

The terms in Eq. (22) correspond to the ones in Eq. (12). All dependencies on the energy, either explicit or implicit in the wave numbers, are shown. Again, setting the underlined terms to zero reduces the open problem to the closed bound-state problem. Note that the coefficient matrix in Eq. (22) is a quadratic function of wavenumber k_L, and $a(E)\mathbf{P}$ depends on the in-coming wave amplitude $a(E)$. Note also that the coefficient matrix is a tridiagonal matrix for the strictly one-dimensional problem. But, for quantum waveguide system with resonantly-coupled cavities, there are branch points which introduce additional matrix elements. We will see that these additional matrix elements are crucial for the eigenvalue problem leading to transmission zeros in Sec. V.

From Eqs. (9a) and (14a), we see that $t(E)$ is related to ψ_n and $r(E)$ is related to ψ_1. By appropriately rearranging the positions of $a(E)$, $t(E)$, and $r(E)$ in Eq. (22), we obtain the formalism for transmission poles, zeros, and ones.

III. NONLINEAR EIGENVALUE PROBLEM FOR TRANSMISSION POLES

In order to find the quasi-bound states of the system, we set the in-coming source flux to zero, $a(E)=0$, as shown in Fig. 1(b). This results in the homogeneous problem derived from Eq. (22) by setting the right-hand side to zero,

$$(\mathbf{H}-k_L\mathbf{B}^L-k_R\mathbf{B}^R-E\mathbf{D})\boldsymbol{\psi}=0. \tag{23}$$

This is a nonlinear eigenvalue problem since it depends both upon energy and the wave number. Solutions only exist for certain values of the energy E, and the corresponding values of k_L and k_R. The complexity of this eigenvalue problem depends upon the relationship between E and k. Within an effective mass model, there is a quadratic relationship between energy E and wave number k, which is given by Eq. (6a).

If we express the energy E in terms of the wave vector in the in-coming lead with wave number k_L, the eigenvalue problem Eq. (23) becomes

$$(\mathbf{A}-k_L\mathbf{B}^L-k_R\mathbf{B}^R-k_L^2\mathbf{C})\boldsymbol{\psi}=0, \tag{24}$$

where

$$\mathbf{A}=\mathbf{H}-F_L\mathbf{D}, \tag{25a}$$

$$\mathbf{C}=\frac{\hbar^2}{2m_L^*}\mathbf{D}. \tag{25b}$$

It is known that the quasi-bound states lead to poles of the transmission amplitude (and the propagator) in the complex-energy plane. This is equivalent to the vanishing of the determinant of the matrix in Eq. (23). The degree of nonlinearity of the eigenvalue problem for k_L (or k_R) depends upon the applied bias. We will show below that for zero bias the resultant eigenvalue problem is of second order, and for finite applied bias of fourth order. These higher-order problems may be reduced to customary linear eigenvalue problems with increased matrix size. The matrix size increases by a factor of two for the second-order case ($V_{\text{bias}}=0$), and by a factor of four for the fourth-order case ($V_{\text{bias}}\neq 0$).

A. Second-order eigenvalue problem for zero bias

Zero bias implies $F_L=F_R$, as shown in Fig. 2(b). We are free to choose the zero of the energy scale such that $F_L=F_R=0$. k_L and k_R now are related by [from Eq. (6a)],

$$\frac{1}{\sqrt{m_R^*}}k_R=\frac{1}{\sqrt{m_L^*}}k_L. \tag{26}$$

We can combine the boundary terms $k_L\mathbf{B}^L$ and $k_R\mathbf{B}^R$ in Eq. (24) into one term $k_L\mathbf{B}$ by defining

$$\mathbf{B}=\mathbf{B}^L+\sqrt{\frac{m_R^*}{m_L^*}}\mathbf{B}^R. \tag{27}$$

Using the definitions of the matrices $\mathbf{B}^L$ and $\mathbf{B}^R$, the elements of $\mathbf{B}$ are given by

$$\mathbf{B}_{ij}=\frac{1}{m_L^*}\delta_{1i}\delta_{1j}+\sqrt{\frac{1}{m_L^*m_R^*}}\delta_{ni}\delta_{nj}. \tag{28}$$

With this, Eq. (24) becomes

$$(\mathbf{A}-k_L\mathbf{B}-k_L^2\mathbf{C})\boldsymbol{\psi}=0. \tag{29}$$

This is a quadratic eigenvalue problem in k_L, which cannot be solved by the standard linear eigenvalue solver routines. Note that the above second-order eigenvalue problem for the quasi-bound states reduces to the usual bound-state eigenvalue problem $(\mathbf{H}-E\mathbf{D})\boldsymbol{\psi}=0$ since the term linear in k_L vanishes and $\mathbf{A}=\mathbf{H}$ and $k_L^2\mathbf{C}=E\mathbf{D}$.

It is possible to linearize the above problem by doubling the matrix dimensions.[11] Writing the identity, $k_L\psi=k_L\psi$ and Eq. (29) as a system yields,

$$\left[\begin{pmatrix}0 & \mathbf{I}\\ \mathbf{A} & -\mathbf{B}\end{pmatrix}-k_L\begin{pmatrix}\mathbf{I} & 0\\ 0 & \mathbf{C}\end{pmatrix}\right]\begin{pmatrix}\boldsymbol{\psi}\\ k_L\boldsymbol{\psi}\end{pmatrix}=0. \tag{30}$$

Using the definitions

$$\mathbf{M}^{(2)}=\begin{pmatrix}0 & \mathbf{I}\\ \mathbf{A} & -\mathbf{B}\end{pmatrix}, \tag{31a}$$

$$\mathbf{N}^{(2)}=\begin{pmatrix}\mathbf{I} & 0\\ 0 & \mathbf{C}\end{pmatrix}, \tag{31b}$$

$$\mathbf{X}^{(2)}=\begin{pmatrix}\boldsymbol{\psi}\\ k_L\boldsymbol{\psi}\end{pmatrix}, \tag{31c}$$

we obtain

$$(\mathbf{M}^{(2)}-k_L\mathbf{N}^{(2)})\mathbf{X}^{(2)}=0. \tag{32}$$

This is a linear eigenvalue problem with twice the matrix size of the original problem, which is contained in the lower half of the system of equations. The upper half is identically zero. For simplicity, the identity matrix $\mathbf{I}$ was chosen for this purpose, but any matrix would do as long as the resultant matrices $\mathbf{M}^{(2)}$ and $\mathbf{N}^{(2)}$ remain nonsingular.

The eigenstates of the system are given as the solutions to the above generalized linear eigenvalue problem with a doubled matrix dimension of $2n$. However, notice that if k_L is an eigenvalue, then its negative complex conjugate $-k_L^*$ is also an eigenvalue.[12] Therefore, we only need to find half of the eigenvalues in problem (32).

B. Fourth-order eigenvalue problem for non-zero bias

We now consider the case of an applied bias voltage V_{bias} between the left and right contacts. We choose the Fermi level on the left as the zero of the energy scale, i.e., $F_L=0$, and consequently $F_R=-eV_{\text{bias}}$. The wave numbers k_L and k_R are related by [from Eq. (6a)],

$$\frac{k_R^2}{m_R^*}+\frac{k_L^2}{m_L^*}=\frac{4}{\hbar^2}E+\frac{2}{\hbar^2}eV_{\text{bias}}, \tag{33a}$$

$$\frac{k_R^2}{m_R^*}-\frac{k_L^2}{m_L^*}=\frac{2}{\hbar^2}eV_{\text{bias}}. \tag{33b}$$

We now express the variables k_L and k_R in terms of a new set of variables k and κ, which are defined by

$$\frac{k_L}{\sqrt{m_L^*}}=k-\kappa, \tag{34a}$$

$$\frac{k_R}{\sqrt{m_R^*}}=k+\kappa. \tag{34b}$$

The nonlinear eigenvalue problem (24) can now be rewritten as

$$[\mathbf{A}-k(\sqrt{m_L^*}\mathbf{B}^L+\sqrt{m_R^*}\mathbf{B}^R)-\kappa(\sqrt{m_R^*}\mathbf{B}^R-\sqrt{m_L^*}\mathbf{B}^L)$$
$$-k^2m_L^*\mathbf{C}+k\kappa 2m_L^*\mathbf{C}-\kappa^2m_L^*\mathbf{C}]\boldsymbol{\psi}=0. \tag{35}$$

Since k_L and k_R are related, k and κ are also related by

$$\kappa=\frac{eV_{\text{bias}}}{2\hbar^2}\frac{1}{k}. \tag{36}$$

We can now replace κ by k in (35). After multiplying the resulting equation by k^2, we obtain a fourth-order eigenvalue problem in k,

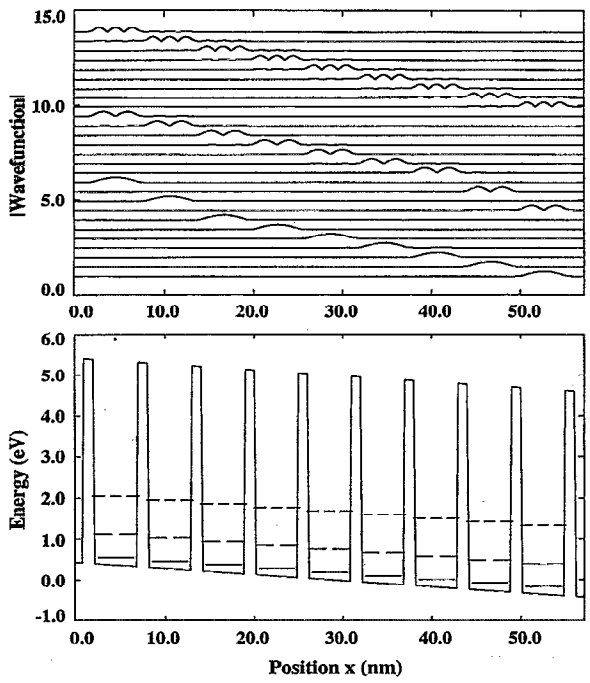

FIG. 3. The quasi-bound states of a multi-barrier resonant tunneling structure in an electric field of $\mathscr{E}=150$ kV/cm. The lower panel shows the potential with the quasi-bound state energies. The states are plotted as horizontal lines at the real energy of the resonance, and the lines are drawn for those positions at which the absolute value of the wave function is larger than a threshold value. The upper panel shows the wave functions over the whole structure, offset for clarity. The corresponding real- and imaginary-parts of the resonant states in each ladder are given in Table I.

$$(\mathbf{A}^{(4)}-k\mathbf{B}^{(4)}-k^2\mathbf{C}^{(4)}-k^3\mathbf{D}^{(4)}-k^4\mathbf{E}^{(4)})\boldsymbol{\psi}=0, \tag{37}$$

where

$$\mathbf{A}^{(4)}=-m_L^*\left(\frac{eV_{\text{bias}}}{2\hbar^2}\right)^2\mathbf{C}, \tag{38a}$$

$$\mathbf{B}^{(4)}=\frac{eV_{\text{bias}}}{2\hbar^2}(\sqrt{m_R^*}\mathbf{B}^R-\sqrt{m_L^*}\mathbf{B}^L), \tag{38b}$$

$$\mathbf{C}^{(4)}=-\left(\mathbf{A}+2m_L^*\frac{eV_{\text{bias}}}{2\hbar^2}\mathbf{C}\right), \tag{38c}$$

$$\mathbf{D}^{(4)}=\sqrt{m_L^*}\mathbf{B}^L+\sqrt{m_R^*}\mathbf{B}^R, \tag{38d}$$

$$\mathbf{E}^{(4)}=m_L^*\mathbf{C}. \tag{38e}$$

In the above expressions, the matrices $\mathbf{A}$, $\mathbf{B}^L$, $\mathbf{B}^R$, and $\mathbf{C}$ are defined in Eq. (24). Note that the fourth-order eigenvalue problem for k in Eq. (37), reduces to the bound state eigenvalue problem for zero bias. For $V_{\text{bias}}=0$, $\mathbf{A}^{(4)}=\mathbf{B}^{(4)}=0$ and $\mathbf{C}^{(4)}=-\mathbf{A}$. Equation (37) becomes $k^2(\mathbf{A}-k\mathbf{D}^{(4)}-k^2\mathbf{E}^{(4)})\boldsymbol{\psi}=0$ which reduces to $(\mathbf{H}-E\mathbf{D})\boldsymbol{\psi}=0$ since the term containing $\mathbf{D}^{(4)}$ vanishes for bound states, $\mathbf{A}=\mathbf{H}$ and $k^2m_L^*\mathbf{C}=E\mathbf{D}$.

Equation (37) is a fourth-order polynomial in k which can be rewritten as

$$\left[\begin{pmatrix} 0 & \mathbf{I} & 0 & 0 \\ 0 & 0 & \mathbf{I} & 0 \\ 0 & 0 & 0 & \mathbf{I} \\ \mathbf{A}^{(4)} & \mathbf{B}^{(4)} & \mathbf{C}^{(4)} & \mathbf{D}^{(4)} \end{pmatrix}-k\begin{pmatrix} \mathbf{I} & 0 & 0 & 0 \\ 0 & \mathbf{I} & 0 & 0 \\ 0 & 0 & \mathbf{I} & 0 \\ 0 & 0 & 0 & \mathbf{E}^{(4)} \end{pmatrix}\right]\times\begin{bmatrix} \boldsymbol{\psi} \\ k\boldsymbol{\psi} \\ k^2\boldsymbol{\psi} \\ k^3\boldsymbol{\psi} \end{bmatrix}=0. \tag{39}$$

Using the definitions

$$\mathbf{M}^{(4)}=\begin{pmatrix} 0 & \mathbf{I} & 0 & 0 \\ 0 & 0 & \mathbf{I} & 0 \\ 0 & 0 & 0 & \mathbf{I} \\ \mathbf{A}^{(4)} & \mathbf{B}^{(4)} & \mathbf{C}^{(4)} & \mathbf{D}^{(4)} \end{pmatrix}, \tag{40a}$$

$$\mathbf{N}^{(4)}=\begin{pmatrix} \mathbf{I} & 0 & 0 & 0 \\ 0 & \mathbf{I} & 0 & 0 \\ 0 & 0 & \mathbf{I} & 0 \\ 0 & 0 & 0 & \mathbf{E}^{(4)} \end{pmatrix}, \tag{40b}$$

$$\mathbf{X}^{(4)}=\begin{pmatrix} \boldsymbol{\psi} \\ k\boldsymbol{\psi} \\ k^2\boldsymbol{\psi} \\ k^3\boldsymbol{\psi} \end{pmatrix}, \tag{40c}$$

we obtain

$$(\mathbf{M}^{(4)}-k\mathbf{N}^{(4)})\mathbf{X}^{(4)}=0. \tag{41}$$

Again, $\mathbf{I}$ is the identity matrix, and it could be replaced by any other matrix that makes the matrices $\mathbf{M}^{(4)}$ and $\mathbf{N}^{(4)}$ nonsingular. Equation (41) is a generalized linear eigenvalue problem with quadrupled dimension of the original matrix.

IV. NONLINEAR EIGENVALUE PROBLEM FOR TRANSMISSION ONES

Transmission ones occur when the reflection amplitude is zero, as can be seen from Fig. 1(c). Therefore, we treat $r(E)$ as the known variable and $a(E)$ as the unknown variable. Moving $r(E)$ [note that $r(E)$ is related to ψ_1] to the right-hand side in problem (22) and forcing it to zero, we obtain an eigenvalue problem for the transmission ones.

From Eqs. (9a) and (14a), we substitute ψ_1 in Eq. (22) in terms of $r(E)$ and $a(E)$. Leaving only terms proportional to $r(E)$ on the right-hand side leads to the following inhomogeneous problem

$$(\mathbf{H}+k_L\mathbf{B}^L-k_R\mathbf{B}^R-E\mathbf{D})\boldsymbol{\psi}=-r(E)\mathbf{P}. \tag{42}$$

It is easy to see that the matrices $\mathbf{H}$, $\mathbf{D}$, $\mathbf{B}^R$, and $\mathbf{B}^L$ are the same as in Eqs. (19–20, 21d), but $\mathbf{P}$ has the new definition,

TABLE I. The calculated quasi-bound state energy ladders from Fig. 3.

First	Second	Third
$0.55-9.8\times10^{-06}i$	$1.11-1.4\times10^{-04}i$	$2.05-8.2\times10^{-04}i$
$0.46-4.8\times10^{-10}i$	$1.02-4.6\times10^{-07}i$	$1.96-2.6\times10^{-05}i$
$0.37-1.6\times10^{-13}i$	$0.93-3.5\times10^{-10}i$	$1.87-2.0\times10^{-07}i$
$0.28-1.7\times10^{-13}i$	$0.84-1.5\times10^{-13}i$	$1.78-6.8\times10^{-10}i$
$0.19-1.3\times10^{-13}i$	$0.75-8.5\times10^{-14}i$	$1.69-2.9\times10^{-11}i$
$0.10-4.8\times10^{-15}i$	$0.66-3.4\times10^{-12}i$	$1.60-5.1\times10^{-09}i$
$0.01-3.1\times10^{-12}i$	$0.57-2.3\times10^{-09}i$	$1.51-6.2\times10^{-07}i$
$-0.08-9.8\times10^{-09}i$	$0.48-1.0\times10^{-06}i$	$1.42-4.1\times10^{-05}i$
$-0.17-1.8\times10^{-05}i$	$0.39-1.6\times10^{-04}i$	$1.32-9.0\times10^{-04}i$

$$\mathbf{P}=e^{-ik_Lx_L}\begin{pmatrix}\left(W_{11}-\dfrac{ik_L}{m_L^*}\right)\\ W_{21}\\ 0\\ \vdots\\ 0\end{pmatrix}, \tag{43}$$

and ψ_1 is related to the now unknown in-coming wave amplitude $a(E)$ by $\psi_1 = a(E)e^{ik_Lx_L}$. Forcing $r(E)=0$ in (42) leads to an eigenvalue problem similar to (23). The solution of this eigenvalue problem follows the same treatment as given in the previous section.

V. NONLINEAR EIGENVALUE PROBLEM FOR TRANSMISSION ZEROS

Transmission zeros occur when the transmission amplitude is zero, as shown in Fig. 1(d). Therefore, we treat $t(E)$ as the known variable and $a(E)$ and $r(E)$ as the unknown variables. Moving $t(E)$ [note that $t(E)$ is related to ψ_n] to the right-hand side in problem (22) and forcing it to zero, we obtain an eigenvalue problem for the transmission zeros.

From Eqs. (9a) and (14a), we substitute ψ_n in (22) in terms of $t(E)$. Rearranging the equation such that only terms proportional to $t(E)$ appear on the right-hand side, leads to the following inhomogeneous problem

$$(\mathbf{H}-k_L\mathbf{B}-E\mathbf{D})\boldsymbol{\psi}=-t(E)\mathbf{P}. \tag{44}$$

Similar to the treatment before, it is easy to see that now $\psi_n = a(E)e^{ik_Lx_L}$ and $\mathbf{W}=(\mathbf{H}-E\mathbf{D})$ is given by

$$\begin{pmatrix} W_{11} & W_{12} & 0 & 0 & 0\\ W_{21} & \ddots & \ddots & 0 & 0\\ 0 & \ddots & \ddots & \ddots & 0\\ 0 & 0 & \ddots & W_{(n-1)(n-1)} & 0\\ 0 & 0 & 0 & W_{n(n-1)} & 0\end{pmatrix}, \tag{45}$$

and the matrices $\mathbf{B}$ and $\mathbf{P}$ have the forms

$$\mathbf{P}=e^{ik_Rx_R}\begin{pmatrix}0\\ 0\\ \vdots\\ W_{(n-1)n}\\ \left(W_{nn}-\dfrac{ik_R}{m_R^*}\right)\end{pmatrix}, \tag{46a}$$

$$\mathbf{B}=\frac{i}{m_L^*}\begin{pmatrix}1 & 0 & 0 & 0 & -2\\ 0 & 0 & \ddots & 0 & 0\\ 0 & \ddots & \ddots & \ddots & 0\\ 0 & 0 & \ddots & \ddots & 0\\ 0 & 0 & 0 & 0 & 0\end{pmatrix}. \tag{46b}$$

Forcing $t(E)=0$ in (44) leads to an eigenvalue problem similar to (23). This problem can be reduced, however, as will be shown.

The matrix on the left-hand side of Eq. (44) is

$$\begin{pmatrix} W_{11}-\dfrac{ik_L}{m_L^*} & W_{12} & 0 & 0 & \dfrac{2ik_L}{m_L^*}\\ W_{21} & \ddots & \ddots & 0 & 0\\ 0 & \ddots & \ddots & \ddots & 0\\ 0 & 0 & \ddots & W_{(n-1)(n-1)} & 0\\ 0 & 0 & 0 & W_{n(n-1)} & 0\end{pmatrix}, \tag{47}$$

which can be reduced by removing the first row and the n(th) column,

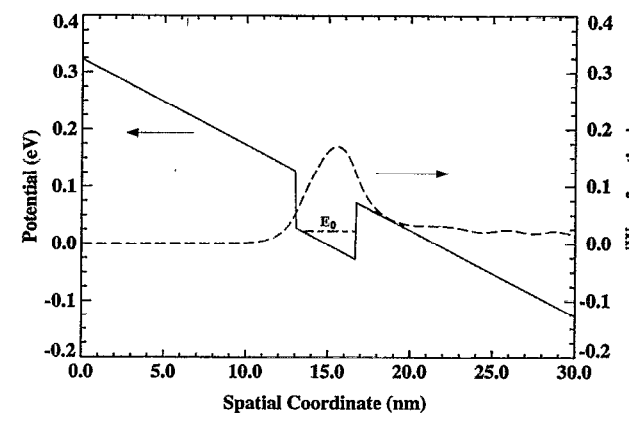

FIG. 4. The potential profile of a single quantum well in a uniform electric field of 150 kV/cm (solid line). The wave function of the first quasi-bound states (dashed line) and its position (dash-dotted line) are also shown.

TABLE II. Comparison of the calculated quasi-bound state energies for a single quantum well with an applied bias.

E(kV/cm)		Phase-shift method (eV)[a]	Stabilization method (eV)[b]	Search method (eV)[c]	Eigenvalue method (eV)[d]
75	E_0	0.025167	0.025167	0.025167	0.025527
	Γ	9.5×10^{-7}	4.3×10^{-6}	9.3×10^{-7}	1.8×10^{-6}
100	E_0	0.024210	0.024211	0.024211	0.024573
	Γ	1.8×10^{-5}	2.0×10^{-5}	1.8×10^{-5}	1.8×10^{-5}
150	E_0	0.021382	0.021170	0.021372	0.021784
	Γ	3.2×10^{-4}	3.3×10^{-4}	3.2×10^{-4}	4.3×10^{-4}

[a]Reference 14.
[b]Reference 15.
[c]Reference 16.
[d]This work.

$$\begin{pmatrix} W_{21} & W_{22} & \ddots & 0 \\ 0 & W_{32} & \ddots & \ddots \\ 0 & 0 & \ddots & W_{(n-1)(n-1)} \\ 0 & 0 & 0 & W_{n(n-1)} \end{pmatrix}. \tag{48}$$

Therefore, the boundary terms which are proportional to k_L and k_R no longer appear in the final problem. The resulting eigenvalue problem is linear in energy.

For a pure one-dimensional problem, Eq. (48) does not have physical solutions [the only solution is $(\mathbf{H}_{(i+1)i}-E\mathbf{D}_{(i+1)i}=0$]. This implies that transmission zeros do not exist in pure one-dimensional resonant tunneling systems, which we know to be true.

For quantum waveguide systems with resonantly-coupled cavities, as was mentioned in Sec. II, there are additional matrix elements in (48). Therefore, in these cases, the corresponding matrix (48) has physical solutions. For the t-stub and loop structures shown in Fig. 2(a), the eigenvalue problem (48) can be further simplified to a real symmetric eigenvalue problem, which only possesses real eigenvalues. This result is consistent with our previous investigation,[13] where we proved that transmission zeros exist on the real-energy axis for t-stub and loop structures.

VI. EXAMPLES

In this section, we apply our eigenvalue method to some model systems to demonstrate its utility. First, we present a multi-barrier resonant tunneling structure with applied external bias. Then, we study a single quantum well structure and a double-barrier resonant tunneling structure. Last, we calculate the positions of transmission poles and zeros in quantum waveguide systems, which include t-stub and loop structures. We compare the results of our direct eigenvalue method to the more conventional method of searching for the zero of the system determinant in the complex-energy plane.

A. Multi-barrier resonant tunneling structure with bias

As our model system, we consider a 10-barrier resonant tunneling structure in an electric field of $\mathscr{E}=150$ kV/cm. Each barrier width and height is 1.0 nm and 5.0 eV, respectively, and the well width is 5.0 nm. For the finite element discretization, we use an average spatial mesh size of 0.2 nm for the numerical calculation, which yields matrices of dimension 286 in Eq. (24). We choose the middle of the structure as the zero point of the potential.

Applying our eigenvalue method to this structure, we obtain the energies of the quasi-bound states, which are the

TABLE III. The first resonant state of two double-barrier resonant tunneling systems obtained by Guo *et al.* and Shao *et al.* The parameters L_b and L_w denote the barrier width and well width, respectively.

Barrier material	L_b(Å)	L_w(Å)	E_1(eV)[a]	E_1(eV)[b]
AlGaAs	50	50	$0.07348-1.95\times10^{-4}i$	$0.07352-2.04\times10^{-4}i$
	45	50	$0.07344-3.60\times10^{-4}i$	$0.07347-3.75\times10^{-4}i$
	40	50	$0.07337-6.50\times10^{-4}i$	$0.07339-6.88\times10^{-4}i$
	35	50	$0.07324-1.20\times10^{-3}i$	$0.07324-1.25\times10^{-3}i$
	30	50	$0.07301-2.25\times10^{-3}i$	$0.07293-2.33\times10^{-3}i$
	25	50	$0.07258-4.20\times10^{-3}i$	$0.07227-4.30\times10^{-3}i$
AlAs	25	45	$0.13712-2.00\times10^{-6}i$	$0.13726-2.20\times10^{-6}i$
	15	45	$0.13799-1.60\times10^{-4}i$	$0.13713-1.80\times10^{-4}i$
	28	62	$0.08524-2.00\times10^{-7}i$	$0.08532-2.00\times10^{-7}i$

[a]Reference 17.
[b]This work.

poles of the transmission amplitude in the complex-energy plane. It is well known that no transmission zeros exist in this case. It is a relatively easy matter to numerically obtain the eigenvalues of the linear system, Eq. (41), with dimension 1,144. The results are plotted in Fig. 3, which shows the resulting Stark ladder structure. The lower panel displays the finite-superlattice potential with the quasi-bound states indicated by the horizontal lines. A line segment is plotted when the wave function is larger than some threshold value, and the upper panel shows the wave functions over the whole structure, offset from each other for clarity. The formation of energy-ladders is evident, which are derived from the individual states in each well, and the complex-energy values are also given in Table I. The imaginary part of each pole gives the inverse of the lifetime for the corresponding quasi-bound state. As one would expect, the longest-lived states are concentrated in the middle of the structure, and states toward the edges are more "leaky." Note that the imaginary parts vary by many orders of magnitude. This makes a direct search for the locations of the poles in the complex-energy plane very costly since a very fine energy mesh has to be used in order to avoid missing poles. In contrast, our direct method yields the energies of all poles, without any search, as the solutions of a linear eigenvalue problem.

B. Single quantum well with bias

In Fig. 4, we show a single quantum well structure in an electric field. The well width and depth are 3.7 nm and 0.1 eV, respectively. This particular structure has been investigated by several researchers.[14–16] Ahn and Chuang[16] have used Airy functions for an exact solution of Schrödinger's equation. By matching the wave functions at the edge of the quantum well, they obtain a secular equation. The quasi-bound states of the system are then found by searching for the zeros of the determinant of this secular equation.

In our treatment here, we model the system to be 30 nm long. We use an average mesh size of 0.2 nm in the calculation, which implies that the matrix size of the linear eigenvalue problem Eq. (41) is 600. We choose the middle of the quantum well as the zero point of the potential. The first quasi-bound state for different biases is: $E_0=(0.025527-1.8\times10^{-6}i)$ eV for $\mathscr{E}=75$ kV/cm, $E_0=(0.024573-1.8\times10^{-5}i)$ eV for $\mathscr{E}=100$ kV/cm, and $E_0=(0.021784-4.3\times10^{-4}i)$ eV for $\mathscr{E}=150$ kV/cm, where $\mathscr{E}$ is the electric field. Table II shows a comparison of our results to those obtained in the other studies.[14–16]

We show the wave function of the first quasi-bound state and its position in Fig. 4 for $\mathscr{E}=150$ kV/cm. The solid line represents the potential profile, the dash-dotted line represents the position of the quasi-bound state, and the dashed line represents the absolute value of the wave function. As one would expect the wave function is slightly tilted to the lower potential region due to the quantum-confined Stark effect.

C. Double-barrier resonant tunneling

We also study two symmetrical double-barrier resonant tunneling systems formed by AlGaAs-GaAs-AlGaAs and AlAs-GaAs-AlAs structures. Guo and co-workers have investigated two specific structures by solving the time independent and time dependent Schrödinger equations.[17] Their calculation (as does ours) accounts for the mass discontinuity, which is $0.067m_0$ for GaAs, $0.09m_0$ for AlGaAs, and $0.15m_0$ for AlAs, where m_0 is the free-electron mass. The barrier height is 0.23 eV for AlGaAs and 1.355 eV for AlAs. Their results of the first resonant state are listed in Table III for different barrier and well widths. Using the same parameters, and spatial mesh dimension of 0.05 nm, we calculated the resonant states of the above systems using our direct eigenvalue method. The results of the first resonant state are also listed in Table III for comparison.

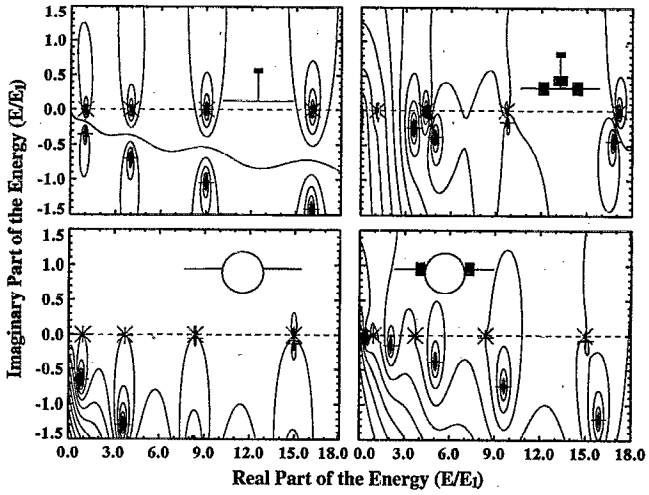

FIG. 5. Contour plots of the absolute value of the transmission amplitude for t-stub and loop structures, which are schematically shown in the insets. The symbols + and × represent the positions of transmission poles and zeros, respectively, which were calculated by our direct eigenvalue method. The energy of the first standing wave in the stub ($E_1=56.1$ meV) is used as the unit of energy.

D. Quantum waveguide structures

We also choose several t-stub and loop structures as our model systems, which are schematically shown in the insets of Fig. 5. The solid lines represent the waveguides which are single-moded transmission channels; generalization to the multi-moded case is possible, yet cumbersome. The shaded boxes represent tunneling barriers (0.5 eV high and 1 nm thick), and the full filled box terminates the stub. For the t-stub structures, the length of the stub is 10 nm and the distance between two tunneling barriers on the main transmission channel is 4 nm. For the asymmetrical loops shown here, the lengths of the two arms are 10 and 11 nm, respectively. Spatial mesh dimensions of 0.2 nm are used in the numerical calculations. It is well known that these systems possess both transmission poles and zeros.[13] The contour lines in Fig. 5 represent the absolute value of the transmission amplitude in the complex-energy plane, which is obtained from a solution of the inhomogeneous problem (22). Poles and zeros, which occur on the real-energy axis, are easily discerned. Using the appropriate eigenvalue problem,

we also show the directly calculated locations of the transmission poles and zeros which are indicated by the + and × symbols, respectively. Note the perfect agreement between the two methods. Again, our technique directly yields poles and zeros without a need to search for them in the complex-energy plane.

VII. SUMMARY

We presented a new approach for directly calculating the positions of transmission poles, ones, and zeros in resonant transmitting systems. In general, a transmission problem is an inhomogeneous problem. Forcing the in-coming source flux to zero results in a nonlinear eigenvalue problem. Using the finite element method, furthermore, these nonlinear eigenvalue problems become linear. It is then an easy matter to directly calculate the energies of the transmission poles, ones, and zeros. This algorithm can be used for systems with arbitrary potential profile, and its utility is demonstrated by applying it to several examples.

ACKNOWLEDGMENT

This work was supported, in part, by the Air Force Office of Scientific Research and the Office of Naval Research.

[1] W. R. Frensley, Rev. Mod. Phys. **62**, 745 (1990).
[2] L. D. Landau and E. M. Lifshitz, *Quantum Mechanics* (Pergamon, New York, 1962).
[3] R. Landauer, IBM J. Res. Develop. **1**, 223 (1957); R. Landauer, Philos. Mag. **21**, 863 (1970).
[4] M. Büttiker, Phys. Rev. Lett. **57**, 1761 (1986).
[5] C. S. Lent and D. J. Kirkner, J. Appl. Phys. **67**, 6353 (1990).
[6] T. B. Bahder, C. A. Morrison, and J. D. Bruno, Appl. Phys. Lett. **51**, 1089 (1987).
[7] G. García-Calderón, Solid State Commun. **62**, 441 (1987); G. García-Calderón, A. Rubio, and R. Romo, J. Appl. Phys. **69**, 3612 (1991).
[8] J. H. Luscombe, Nanotechnology **4**, 1 (1993).
[9] W. R. Frensley, Superlattices and Microstructures **11**, 347 (1992); C. L. Fernando and W. R. Frensley, J. Appl. Phys. **76**, 2881 (1994).
[10] E. B. Becker, G. F. Carey, and J. T. Oden, *Finite Elements* (Prentice Hall, Englewood Cliffs, NJ, 1981).
[11] J. Lysmer and R. L. Kuhlmeyer, J. Engineer. Mechanics Div. (ASCE) **95**, 859 (1969).
[12] Taking the complex conjugate of Eq. (29) yields $[\mathbf{A}-(-k_L^*)\mathbf{B}-(-k_L^*)^2\mathbf{C}]\psi^*=0$, where we have used that **A** and **C** are real matrices and **B** is purely imaginary. We see that if (k_L,ψ) is an eigen-pair of Eq. (29), then so must be $(-k_L^*,\psi^*)$.
[13] W. Porod, Z. Shao, and C. S. Lent, Appl. Phys. Lett. **61**, 1350 (1992); Z. Shao, W. Porod, and C. S. Lent, Phys. Rev. B **49**, 7453 (1994).
[14] E. J. Austin and M. Jaros, Appl. Phys. Lett. **47**, 274 (1985).
[15] F. Borondo and J. Sanchez-Dehesa, Phys. Rev. B **33**, 8758 (1986).
[16] D. Ahn and S. L. Chuang, Phys. Rev. B **34**, 9034 (1986).
[17] H. Guo, K. Diff, G. Neofotistos, and J. D. Gunton, Appl. Phys. Lett. **53**, 131 (1988).

Journal of Applied Physics is copyrighted by the American Institute of Physics (AIP). Redistribution of journal material is subject to the AIP online journal license and/or AIP copyright. For more information, see http://ojps.aip.org/japo/japcr/jsp
Copyright of Journal of Applied Physics is the property of American Institute of Physics and its content may not be copied or emailed to multiple sites or posted to a listserv without the copyright holder's express written permission. However, users may print, download, or email articles for individual use.